LESION DETECTION USING T1-WEIGHTED MRI: A NEW APPROACH BASED ON FUNCTIONAL CORTICAL ROIS

Dazhou Guo, Kang Zheng, Song Wang

University of South Carolina, Department of Computer Science & Engineering
301 Main St., Columbia, SC, 29208, USA

ABSTRACT

Accurate and precise detection of brain lesions on MR images is important for relating lesion locations to impaired behaviors. In this paper, we propose a method to detect lesion voxels on each functional cortical ROI (Region of Interest) independently using only T1-weighted MR images (T1-MRI). In contrast to existing automatic lesion detection methods, which typically detect lesion voxels on the whole MR image or on gray matter (GM)/white matter (WM), we show that the proposed functional cortical ROI based method can lead to better lesion-detection performance. We evaluate the proposed method using an in-house dataset with 60 chronic stroke patients. Using leave-one-subject-out cross validation, the proposed method can achieve an average Dice coefficient of 0.74 ± 0.11 and outperform three state-of-the-art methods by more than 0.05.

Index Terms— Lesion Detection, Functional Cortical ROIs, T1-weighted MRI, Stacked Autoencoder

1. INTRODUCTION

Accurate detection of lesions in brains is critical to both clinical practice and neuropsychological research. The identification and analysis of the brain lesions resulting from a stroke can help understand the lesion-deficit relationship [1, 2, 3], and chart the development of brain pathology over time. In the past two decades, many lesion detection methods on Magnetic Resonance Imaging (MRI) have been developed and they can generally be categorised into unsupervised methods [4, 5, 6, 7, 8] and supervised methods [9, 10, 11, 12, 13]. Unsupervised methods do not require an annotated data set for training. Lesions are detected as an outlier class by using clustering methods [5] or dictionary learning/sparse coding to model healthy tissues [14]. Supervised methods typically take a training step on a set of annotated data with ground-truth lesions. The data are used to train a classifier, which is then used to detect lesions in new unseen data. While lesion detection can be performed on a combination of different MR imaging modalities [10, 6, 12], i.e., T1-weighted, T2-weighted, Diffusion-weighted, Proton Density-weighted, FLuid Attenuation Inverse Recovery MR images, this paper is focused on lesion detection on a single modality of T1-MRI, considering the additional time and cost in acquiring multiple modality data in practice [5]. Lesion detection on T1-MRI is a well-known challenging problem due to 1) the intensity similarity between lesions and the surrounding healthy tissues, 2) the large variation of the lesion size, shape and location, and 3) the possible brain atrophy [15, 16] that leads to the deformation of the healthy tissues.

Most of the existing lesion detection methods are performed on the entire brain or on GM/WM by labelling each voxel as either lesion or healthy tissue. Stamatakis et al. [4] detect lesion voxels on the whole brain by comparing patient T1-MRI with a set of healthy control images using Markov Random Field. Seghier et al. [5] introduce an unsupervised segmentation method to detect lesion voxels in GM and WM separately, and then group detected lesion voxels to obtain the whole brain lesion. Sanjun et al. [7] adapt the work in [5], and detect lesion voxels in GM and WM separately by introducing an iterative procedure to refine the detected lesion voxels. Guo et al. [13] detect lesion voxels on the whole brain by combining both unsupervised and supervised methods. Under the assumption that the same functional cortical ROI will show similar anatomical patterns/features (i.e., gyri/sulci) across different subjects, we propose a new approach to independently register and segment each functional cortical ROI and detect lesions on each segmented functional cortical ROI. In the remainder of the paper, we abbreviate functional cortical ROI as ROI, when there is no ambiguity. We find that this ROI based approach can produce competitive lesion detection performance than the existing state-of-the-art methods.

Specifically, we propose an ROI segmentation algorithm for T1-MRI, and an unsupervised features learning procedure for each voxel, followed by a supervised classifier training/testing procedure for lesion detection on each ROI. Section 2 discusses the proposed approach in detail, and the experiment results are reported and discussed in Section 3, followed by a brief conclusion in Section 4.

2. METHODS

The proposed approach consists of two components. First, we introduce an algorithm to register and segment each ROI

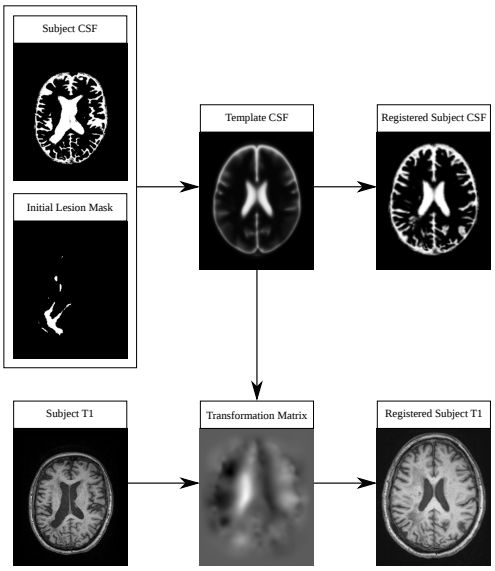

Fig. 1. An illustration of CSF based initial registration.

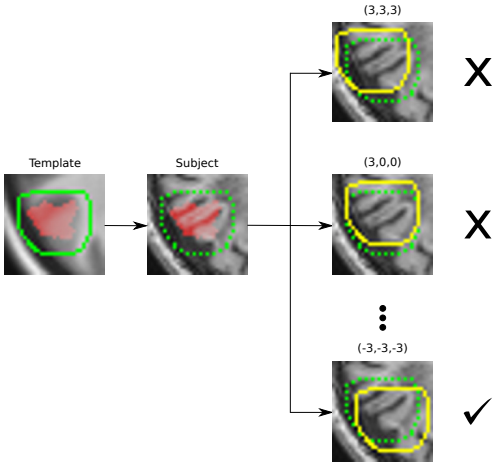

Fig. 2. An illustration of a dilated ROI and its refinements by locally translating its boundary, where highlights using red, green and yellow denote the initial ROI, the initial boundary of the dilated ROI, and the translated boundary of the dilated ROI, respectively.

from an input T1-MRI. Second, on each registered and segmented ROI, we unsupervisedly learn features for each voxel, and then classify each voxel to be lesion or not, followed by a simple grouping procedure to obtain the whole brain lesion detection.

2.1. Functional ROI Segmentation in Lesion Brain

To get ROIs on a subject image, we register the subject T1-MRI to the template (where ROIs are predefined) using SPM12 [17]. Taking advantage of the fact that SPM12 segmentation pipeline is robust in segmenting Ventricles (which are parts of the brain CSF) [18], we use the segmented Ventricles from SPM12 segmentation pipeline to help ROI registration and segmentation. The detailed SPM12 parameter settings will be reported in Section 3.2. Specifically, the proposed ROI segmentation procedure consists of two main steps: 1) an initial ROI detection through CSF based whole brain registration; and 2) an ROI refinement through dilation and local optimal search.

Initial ROI detection through CSF based whole brain registration. As shown in Fig. 1, we first register the subject Ventricles and the outer CSF to the template while masking out the possible lesion regions by introducing a subject-specific initial lesion mask, which will be discussed in the later paragraph. Then, the transformation matrix is used to yoke the original subject T1-MRI into the template.

The subject-specific initial lesion mask is generated using Algorithm 1, where $\mathbf{v} = [x, y, z]$ denotes the location of the voxel in 3D MRI, $\bar{P}_{GM}(\mathbf{v})$ and $P_{GM}(\mathbf{v})$ denote the GM probability of the template and subject at voxel $\mathbf{v}$, and $\bar{P}_{WM}(\mathbf{v})$ and $P_{WM}(\mathbf{v})$ denote the WM probability of the template and subject at voxel $\mathbf{v}$. Note that lesion would be mis-segmented as CSF or GM using SPM12 segmentation pipeline on T1-MRIs [18, 19]. Hence, in the lesion regions, it may show abnormally low probability in P_{WM} and abnormally high/low probability in P_{GM}. Similar to [5], we calculate the voxel-wise difference between subject and template using "tanh" function. In this paper, for generating subject-specific initial lesion masks, we heuristically select $\alpha = 0.6$ and $\lambda = 0.6$, where α is the confidence parameter and λ is the threshold parameter.

Input : $\bar{P}_{GM}, P_{GM}, \bar{P}_{WM}, P_{WM}$
Output: Initial lesion mask L
for *every voxel at* $\mathbf{v}$ **do**

$$L_{GM}(\mathbf{v}) = \text{abs}\left(\tanh\left(\frac{\bar{P}_{GM}(\mathbf{v}) - P_{GM}(\mathbf{v})}{\alpha}\right)\right)$$

$$L_{WM}(\mathbf{v}) = \tanh\left(\frac{\bar{P}_{WM}(\mathbf{v}) - P_{WM}(\mathbf{v})}{\alpha}\right)$$

  if $L_{WM}(\mathbf{v}) > 0$ **then**
    if $\max(L_{GM}(\mathbf{v}), L_{WM}(\mathbf{v})) > \lambda$ **then**
      $L(\mathbf{v}) = 1$
    else
      $L(\mathbf{v}) = 0$
    end
  end
end

Algorithm 1: Algorithm for the initial lesion mask.

ROI refinement through dilation and local optimal search. As shown in Fig. 2, we dilate each ROI, so that we can make sure that all ROIs are either overlapped or adjacent, where red region denotes the ROI and green contour denotes the dilated ROI. In this paper, let $\bar{R}^i$ and R^i denote the i^{th} dilated ROI on the template and subject T1-MRI respectively. Specifically, we can translate the boundary of dilated ROI

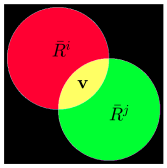

Fig. 3. The red and green circles denote two dilated synthetic ROIs $\bar{R}^i$ and $\bar{R}^i$ in the template.

R^i by an offset $\Delta_i = (\Delta_i x, \Delta_i y, \Delta_i z)$ to get a new region $R^i(\Delta_i)$, as indicated by yellow contours, and then search for an optimal offset Δ_i^*. Using Eq. (1), we can find a refined i^{th} dilated ROI $R^i(\Delta_i^*)$ of the object that best matches to its corresponding dilated ROI $\bar{R}^i$ of the template, i.e.,

$$\Delta_i^* = \arg\min_{\Delta_i} \parallel R^i(\Delta_i) - \bar{R}^i \parallel_2 \quad . \tag{1}$$

In this paper, we abbreviate refined and dilated ROIs as RROIs, when there is no ambiguity. In the next section, we will introduce an unsupervised feature learning method, followed by a classifier for lesion voxel detection in each RROI.

2.2. Model Training and Lesion Voxels Grouping

In this paper, we take each voxel as a sample, and unsupervisedly learn features for each voxel, and then classify each voxel to be lesion or not. The positive samples are the annotated lesion voxels of the patients, and the negative samples are the voxels of healthy controls. At each location $\mathbf{v}$ in the template, we train classifiers $\{C^i_{\mathbf{v}} | \mathbf{v} \in \bar{R}^i \ \& \ i \in \{1, 2, \cdots, n\}\}$, where n is the number of pre-defined ROIs in the template. If $\mathbf{v}$ belongs to only one dilated ROI, e.g., $\bar{R}^i$, there will be only one classifier $C^i_{\mathbf{v}}$. If $\mathbf{v}$ belongs to multiple dilated ROIs, multiple classifiers will be trained, e.g., in Fig. 3, $\mathbf{v} \in \bar{R}^i \cap \bar{R}^j$, and at $\mathbf{v}$ two classifiers $C^i_{\mathbf{v}}$ and $C^j_{\mathbf{v}}$ will be trained.

Considering that lesion voxels are randomly distributed in the brain, for training classifier $C^i_{\mathbf{v}}$, positive samples are constructed using *all annotated lesion voxels* of the patients; yet, the negative samples are constructed using the voxels located at the same $\mathbf{v}$ in $R^i(\Delta_i^*)$. In the following, we will discuss initial feature definition, feature refinement using unsupervised learning and classifier training in details.

Initial feature definition. We define the initial features using the intensity of the corresponding voxel and its neighbours. Specifically, we crop three $5 \times 5 \times 5$ blocks [13], centered at voxel located at $\mathbf{v}$, from T1-MRI and the probability maps of GM and WM respectively, which are then concatenated as the initial features. **Feature refinement using unsupervised learning**. The initial features can be refined using an unsupervised feature learning method. We separately learns the refined features of the positive/negative samples using the initial features of the positive/negative samples. The stacked autoencoder is used for unsupervised feature refinement, the detailed parameter settings will be reported in Section 3.2. **Classifier training procedure**. For each ROI and RROI, we collect its positive and negative training samples as mentioned before and train an ROI-based and an RROI-based classifier, respectively. This way, we obtain one classifier for each ROI and RROI. The softmax classifier is applied for classification. **Classification and grouping procedure**. In detecting lesions for an unseen subject T1-MRI, we first register and segment each ROI and RROI of the subject against the template. For each voxel, we identify the ROI and RROI it belongs to and then use the corresponding pre-trained ROI-based and RROI-based classifiers to classify voxel located at $\mathbf{v}$. We use a majority voting procedure [20] to decide the final classification of this voxel of being lesion or not when the voxel is classified by using multiple classifiers.

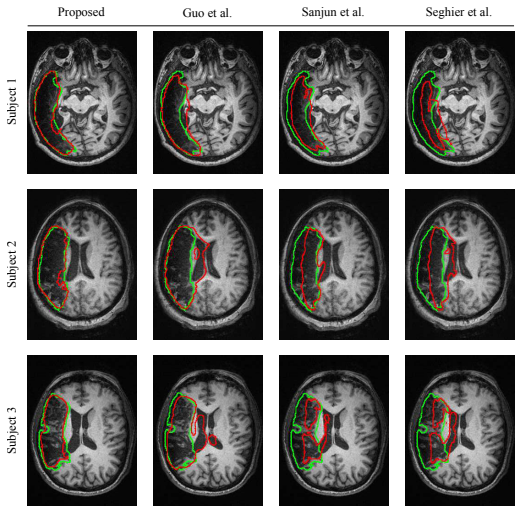

Fig. 4. Sample results of lesion detection using the proposed method and the three comparison methods [13], [7], and [5]. Red and green contours indicate the detected lesion boundaries and the ground-truth lesion boundaries, respectively.

3. EXPERIMENTS

3.1. Experiment Data & Evaluation Metrics

We collected an in-house MRI dataset for our experiment. The templates used in the paper are averaged healthy control T1 template and 136-ROI Neuromorphometrics template from SPM12 toolbox.

We evaluate the performance of the proposed method using a leave-one-out cross validation strategy. All the performance measures are averaged over all the 60 testing rounds. For the evaluation criteria, we follow [5] using Precision, Recall, and Dice coefficient.

Method	Precision	Recall	Dice
Seghier et al. [5]	0.47±0.17	0.54±0.15	0.50±0.15
Sanjun et al. [7]	0.52±0.16	0.60±0.13	0.55±0.13
Guo et al. [13]	0.71±0.15	0.70±0.13	0.69±0.11
Proposed method	**0.75±0.14**	**0.73±0.13**	**0.74±0.11**

Table 1. Performance of the proposed method and comparison methods on the in-house dataset.

α	λ	Precision	Recall	Dice
0.2	0.5	0.16 ± 0.11	$\mathbf{0.92 \pm 0.14}$	0.25 ± 0.11
	0.6	0.19 ± 0.11	0.90 ± 0.15	0.28 ± 0.11
	0.7	0.22 ± 0.12	0.86 ± 0.16	0.32 ± 0.13
	0.8	0.18 ± 0.13	0.81 ± 0.18	0.38 ± 0.14
0.4	0.5	0.28 ± 0.13	0.81 ± 0.18	0.38 ± 0.14
	0.6	0.40 ± 0.16	0.73 ± 0.19	0.47 ± 0.16
	0.7	0.59 ± 0.21	0.64 ± 0.16	0.56 ± 0.18
	0.8	0.80 ± 0.24	0.50 ± 0.10	0.57 ± 0.18
0.6	0.5	0.54 ± 0.20	0.66 ± 0.19	0.54 ± 0.17
	0.6	0.76 ± 0.24	0.54 ± 0.19	$\mathbf{0.58 \pm 0.18}$
	0.7	0.83 ± 0.24	0.38 ± 0.16	0.49 ± 0.18
	0.8	$\mathbf{0.95 \pm 0.25}$	0.19 ± 0.10	0.30 ± 0.14

Table 2. The segmentation performance by only using the inital lesion mask under different α and λ.

3.2. Implementation Details

In Section 2.1, the parameter settings for SPM12 tissue segmentation pipeline are: light bias regularization, FWHM=$60mm$, light clean up, and $3mm$ sampling distance. The parameter settings for ANTs masked registration pipeline are: cross correlation metric $r = 4$, and the spline distance $s = 26$.

In Section 2.2, a two-layer stacked autoencoder with a softmax layer to classify lesion voxels is trained. The parameter settings for the first layer of the stacked autoencoder are: Hidden Size is 50, Max Epoch is 3000. The parameter settings for the second layer of the stacked autoencoder are: Hidden Size is 25, Max Epoch is 1000. The parameter settings for the softmax layer are: Max Epochs is 400. The overall network is fine-tuned using only training dataset.

3.3. Results and Discussion

First, from Table 1, the proposed method achieves a substantially better lesion detection performance (Dice coefficient) than the other methods in terms of all three evaluation criteria. Fig. 4 qualitatively show the detected lesions on selected 2D slices of different patients.

Second, we study the parameter selection for generating the initial lesion masks using Algorithm 1 in Section 2.1. As shown in Table 2, we heuristically select $\alpha = 0.6$ and $\lambda = 0.6$ that can produce the best Dice coefficient for generating the initial lesion mask.

Third, we evaluate the impact of *initial ROI detection through CSF based whole brain registration* and *ROI refinement through dilation and local optimal search* in terms of the final lesion detection's precision, recall and Dice coefficient. We conduct three additional experiments: 1) lesion detection without using the ROI- or RROI-based classifiers; 2) lesion detection using only the ROI-based classifiers; and 3) lesion detection using only the RROI-based classifiers, followed by majority voting. As shown in Table 3, by combining both ROI-based and RROI-based classifiers, followed by majority voting, the proposed method can achieve the best performance.

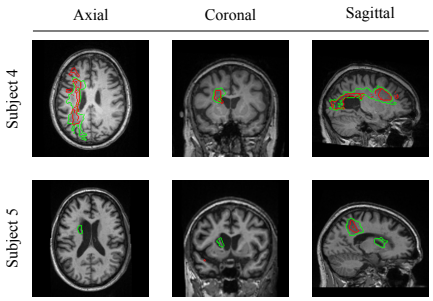

Fig. 5. Two failure cases of lesion detection.

Finally, we discuss the failure cases of the proposed method. As shown in the first row of Fig. 5, the proposed method may fail to detect lesion when the voxel intensity of lesion is very similar to the voxel intensity of WM in T1-MRI. The proposed method may also fail to detect lesions when the lesion is relatively small.

Initial ROI	ROI Refine	Precision	Recall	Dice
×	×	0.70±0.15	0.69±0.13	0.69±0.12
✓	×	0.72±0.15	0.69±0.13	0.70±0.11
×	✓	0.71±0.15	0.71±0.13	0.71±0.11
✓	✓	**0.75±0.14**	**0.73±0.13**	**0.74±0.11**

Table 3. Lesion detection performance w/o initial ROI detection, and w/o the ROI refinement.

4. CONCLUSION

In this paper, we have introduced a new method for automatic lesion detection based on functional cortical ROI using only T1-MRIs. The proposed method first segments the ROI, and then, classifies each voxel in the ROIs using the pre-trained classifiers. In comparison to other state-of-the-art methods, our method achieve improvements in Precision, Recall and Dice coefficient.

5. ACKNOWLEDGEMENT

This work was supported in part by UES Inc./AFRL-S-901-486-002, NSF-1658987, NSFC61672376 and NCPTT-P16AP00373. We thank Hongkai Yu, Hao Guo, Alexandra Basilakos and Julius Fridriksson who provided insight and expertise that greatly assisted the research.

6. REFERENCES

[1] J. Fridriksson, D. Guo, P. Fillmore, A. Holland, and C. Rorden, "Damage to the anterior arcuate fasciculus predicts non-fluent speech production in aphasia," *Brain*, vol. 136, pp. 3451–60, 2013.

[2] A. Basilakos, P. Fillmore, C. Rorden, D. Guo, L. Bonilha, and J. Fridriksson, "Regional white matter damage predicts speech fluency in chronic post-stroke aphasia," *Frontiers in human neuroscience*, vol. 8, pp. 845, 2014.

[3] J. Fridriksson, P. Fillmore, D. Guo, and C. Rorden, "Chronic broca's aphasia is caused by damage to broca's and wernicke's areas," *Cerebral Cortex*, vol. 25, no. 12, pp. 4689–4696, 2015.

[4] E. A. Stamatakis and L. K. Tyler, "Identifying lesions on structural brain images-validation of the method and application to neuropsychological patients," *Brain and Lang*, vol. 94, pp. 167–77, 2005.

[5] M. L. Seghier, A. Ramlackhansingh, J. Crion, A. P. Leff, and C. J. Price, "Lesion identification using unified segmentation-normalization models and fuzzy clustering," *NeuroImage*, vol. 41, pp. 1253–66, 2008.

[6] H. K. Ong, D. Ramachandram, R. Mandava, and I. L. Shuaib, "Automatic white matter lesion segmentation using an adaptive outlier detection method," *NeuroImage*, vol. 30, pp. 807–23, 2012.

[7] A. Sanjun, C. J. Price, L. Mancini, G. Josse, A. Grogan, and A. K. Yamamoto, "An improved lesion detection approach based on similarity measurement between fuzzy intensity segmentation and spatial probability maps," *Magn Reson Imaging*, vol. 28, pp. 245–54, 2013.

[8] H. Yu and X. Qi, "Unsupervised cosegmentation based on superpixel matching and fastgrabcut," in *IEEE International Conference on Multimedia and Expo*, 2014, pp. 1–6.

[9] P. Anbeek, K. L Vicken, M. J. Van Osch, R. H. Bisschops, and J. Van der Ground, "Automatic segmentation fo different-sized white matter lesions by voxel probability estiatmion," *Med Image Anal*, vol. 8, pp. 205–15, 2004.

[10] E. Geremia, B. H. Menze, O. Clatz, E. Konukoglu, A. Criminisi, and N. Ayache, "Spatial decision forests for ms lesion segmentation in multi-channel mr images," *MICCAI*, vol. 6361, pp. 111–8, 2010.

[11] B. A. Abdulah, A. A. Younis, and N. M. John, "Multi-sectional views textural based svm for ms lesion segmentation in multi-channels mris," *The Open Biomed Eng J*, vol. 6, pp. 56–72, 2012.

[12] J. B. Fiot, L. D. Cohen, P. Raniga, and J. Fripp, "Efficient brain lesion segmentation using multi-modality tissue-based feature selection and support vector machines," *Int J Numer Methods in Biomed Eng*, vol. 29, pp. 905–15, 2013.

[13] D. Guo, J. Fridriksson, P. Fillmore, C. Rorden, H. Yu, K. Zheng, and S. Wang, "Automated lesion detection on mri scans using combined unsupervised and supervised methods," *BMC Med Imaging*, vol. 30, pp. 15–50, 2015.

[14] N. Weiss, D. Rueckert, and A. Rao, "Multiple sclerosis lesion segmentation using dictionary learning and sparse coding," *MICCAI*, vol. 8149, pp. 735–42, 2013.

[15] I. Aprile, F. Iaiza, A. Lavaroni, R. Budai, P. Dolso, C. A. Scott, C. A. Beltrami, and G. Fabris, "Analysis of cystic intracranial lesions performed with fluid-attenuated inversion recovery mr imaging," *AJNR Am J Neuroradiol*, vol. 20, pp. 1259–67, 1999.

[16] C. Rorden and M. Brett, "Stereotaxic display of brain lesions," *Behav Neurol*, pp. 191–200, 2000.

[17] K. J. Priston, A. P. Holmes, K. J. Worsley, J. B. Poline, C. D. Frith, and R. S. J. Frackowiak, "Statistical parametric maps in functional imaging: a general linear approach," *Hum Brain Mapp*, pp. 189–210, 1995.

[18] I. B. Malone, K. K. Leung, S. Clegg, J. Barnes, J. L. Whitwell, J. Ashburner, N. C. Fox, and G. R. Ridgway, "Accurate automatic estimation of total intracranial volume: A nuisance variable with less nuisance," *Neuroimage*, pp. 366–72, 2015.

[19] E. Roura, A. Oliver, M. Cabezas, S. Valverde, D. Pareto, J. C. Vilanova, L. Ramio-Torrenta, A. Rovira, and X. Llado, "An spm12 extension for multiple sclerosis lesion segmentation," *SPIE Medical Imaging*, 2015.

[20] P. Viola and M. Jones, "Rapid object detection using a boosted cascade of simple features," *CVPR*, vol. 1, no. 9, pp. I–511, 2001.